THE JOURNAL OF PHYSICAL CHEMISTRY LETTERS
A JOURNAL OF THE AMERICAN CHEMICAL SOCIETY

pubs.acs.org/JPCL Letter

Impact of Geometric Phase on Dynamics of Complex-Forming Reactions: $H + O_2 \rightarrow OH + O$

Junyan Wang, Changjian Xie,* Xixi Hu,* Hua Guo,* and Daiqian Xie*

Cite This: *J. Phys. Chem. Lett.* 2024, 15, 4237−4243 Read Online

ACCESS | Metrics & More | Article Recommendations | Supporting Information

ABSTRACT: Reaction dynamics on the ground electronic state might be significantly influenced by conical intersections (CIs) via the geometric phase (GP), as demonstrated for activated reactions (i.e., the $H + H_2$ exchange reaction). However, there have been few investigations of GP effects in complex-forming reactions. Here, we report a full quantum dynamical study of an important reaction in combustion ($H + O_2 \rightarrow OH + O$), which serves as a proving ground for studying GP effects therein. The results reveal significant differences in reaction probabilities and differential cross sections (DCSs) obtained with and without GP, underscoring its strong impact. However, the GP effects are less pronounced for the reaction integral cross sections, apparently due to the integral of the DCS over the scattering angle. Further analysis indicated that the cross section has roughly the same contributions from the two topologically distinct paths around the CI, namely, the direct and looping paths.

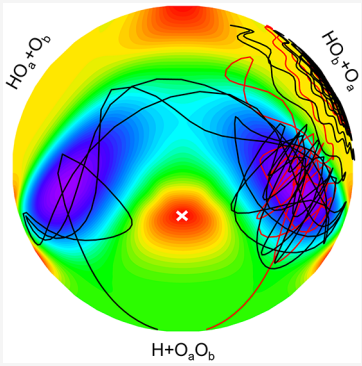

Downloaded via NANJING UNIV on May 6, 2024 at 07:41:55 (UTC).
See https://pubs.acs.org/sharingguidelines for options on how to legitimately share published articles.

The endothermic $H + O_2 \rightarrow OH + O$ reaction is one of the most important elementary steps in gas-phase hydrocarbon combustion, responsible for chain branching during the oxidation of hydrogen.[1] Due to the existence of a deep HO_2 well in the reaction pathway,[2] it also serves as a prototype for complex-forming reactions.[3] For these reasons, this reaction was extensively investigated. Experimentally, its kinetics and dynamics were studied by several groups.[4−13] These experimental studies were complemented by numerous theoretical studies.[14−48] Despite extensive work, a complete understanding of this important process has not been achieved.

A key unresolved issue is that although the reaction nominally proceeds on its electronic ground state (X^2A'') potential energy surface (PES), the dynamics might be influenced by the first excited (A^2A'') state, because of a common type of electronic degeneracy, namely conical intersections (CIs), between these two states, as shown in Figure 1(a). For an N-dimensional system, a CI is an N-2-dimensional cone-shaped seam of degeneracy.[49,50] For the HO_2 system, the branching space is spanned by the $H-O_2$ distance (R) and the Jacobi angle (γ). The two states are coupled near the crossing seams by derivative coupling, which enters the kinetic energy operator as a vector potential in the adiabatic representation.[51] Interestingly, the adiabatic ground state electronic wave function changes its sign along a loop encircling a CI, leading to the so-called geometric phase (GP) in the nuclear wave function,[52] which is related to the Berry's phase.[53] Especially, the wave function acquires a phase (π) each time the system loops around the CI, regardless of the actual path. As a result, two paths passing the CI on different sides might interfere, resulting in a significant impact on quantum dynamics, even when the energy is below the crossing seam.[54−58] Hence, ignoring the GP in the adiabatic treatment of the dynamics could lead to significant errors.[59,60] The GP effect has recently been observed experimentally for the activated $H + HD \rightarrow D + H_2$ reaction,[61] which is affected by a high-energy CI, confirming a theoretical prediction made a long time ago.[51] However, the GP has been ignored in all previous quantum scattering investigations of the complex-forming $H + O_2$ reaction, as only the ground electronic state PES was used in such calculations.[21−24,26−32,34−38,41−44,47,48] Interestingly, earlier quantum dynamics studies of the $H + O_2$ inelastic scattering have revealed significant GP effects.[62−64] Since the complex-forming nature of this reaction differs markedly from that of the direct $H + H_2$ reaction in the dynamics that are strongly influenced by metastable resonances,[3] the impact of GP might also be quite distinct. Already, GP was found to be important for the reverse OH + O reaction at ultracold temperatures.[65−67]

The inclusion of the GP effect in the adiabatic representation by adding the vector potential is numerically difficult, because the derivative coupling and the related diagonal Born−Oppenheimer correction are singular at the crossing seam.[68] Instead, the use of a diabatic representation, in which derivative coupling is removed,[69] is preferred as the

Received: March 14, 2024
Revised: April 8, 2024
Accepted: April 10, 2024
Published: April 11, 2024

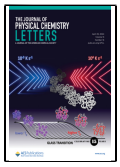

ACS Publications © 2024 American Chemical Society

https://doi.org/10.1021/acs.jpclett.4c00789
J. Phys. Chem. Lett. 2024, 15, 4237−4243

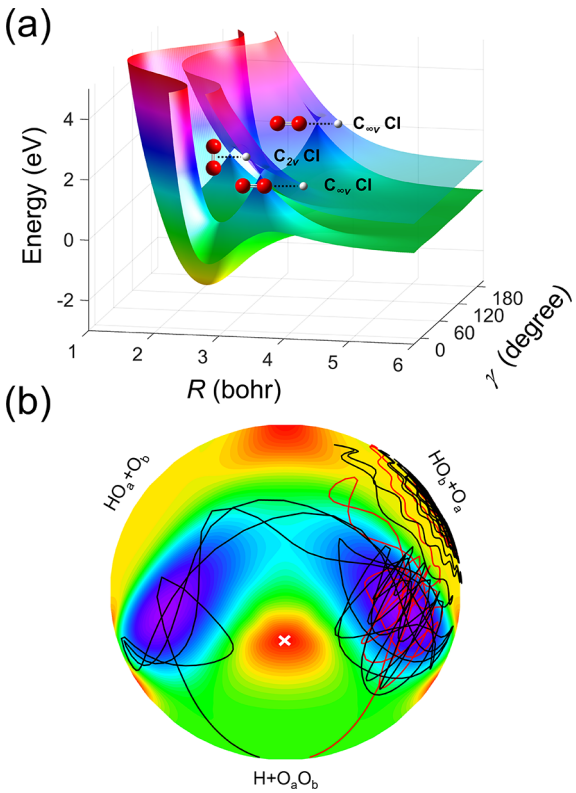

Figure 1. (a) The ground and excited state adiabatic PESs of the HO_2 system in reactant Jacobi coordinates with r_{OO} fixed at 2.28 bohr. Two equivalent linear CIs and a T-shaped CI are clearly seen between the two adiabatic states. (b) Relaxed triangular plot in hyperspherical coordinates of the ground state PES, with the cross for the C_{2v} CI. Exemplary direct (red) and looping (black) trajectories are also shown. (The trajectories were calculated for H + O_2 (v = 0, j = 1) at E_c = 0.70 eV with zero impact parameter.)

GP effect is naturally included with the multistate framework.[70] Unfortunately, rigorous diabatization is not possible for systems with more than two atoms,[71,72] but the residual derivative coupling can be minimized in a so-called quasi-diabatic representation.[73] Diabatization is the determination of the unitary adiabatic-to-diabatic (AtD) transformation that converts the diagonal adiabatic PESs into a diabatic potential energy matrix (DPEM), in which the diagonal and off-diagonal elements are all smooth functions of the nuclear coordinates, thus amenable to analytical representation.[74,75] Recently, we developed a two-state DPEM for the title reaction at the multireference configuration interaction with Davidson correction (MRCI+Q) level with a large basis set.[76] This machine-learned high-fidelity DPEM based on ab initio data is expected to be more accurate than the existing one based on the diatom-in-molecule (DIM) form,[25] thus providing a reliable platform for quantum characterization of the reaction dynamics to unravel the impact of the CIs in this key complex-forming reaction.

Here, we report the first nonadiabatic quantum dynamics study of the H + O_2 (v = 0, j = 1) → OH + O reaction based on our new DPEM, along with adiabatic results for comparison. Such calculations are extremely challenging because of the large basis set needed to cover the vast phase space accessed by the reaction. The total reactive integral cross sections (ICSs) at collision energies (E_c) below 0.80 eV and the differential cross section (DCS) at E_c = 0.70 eV are obtained. The comparison of the nonadiabatic and adiabatic results provides valuable insight into the role of the GP in reactive scattering dominated by long-lived resonances.

To unravel the influence of the GP on the reactive dynamics, we performed both adiabatic and diabatic calculations using the Chebyshev propagator,[77] with details of our quantum dynamics given in the Supporting Information (SI). Since the adiabatic calculation ignores the GP effect, the results will be denoted below as NGP. Analogously, the diabatic calculations include the GP effect and will be denoted as GP. The wave functions in the diabatic and adiabatic representations are connected with each other by the unitary AtD transformation,[74] which is also defined in the SI.

The total reaction probability of the title reaction as a function of the collision energy is displayed in Figure 2 for

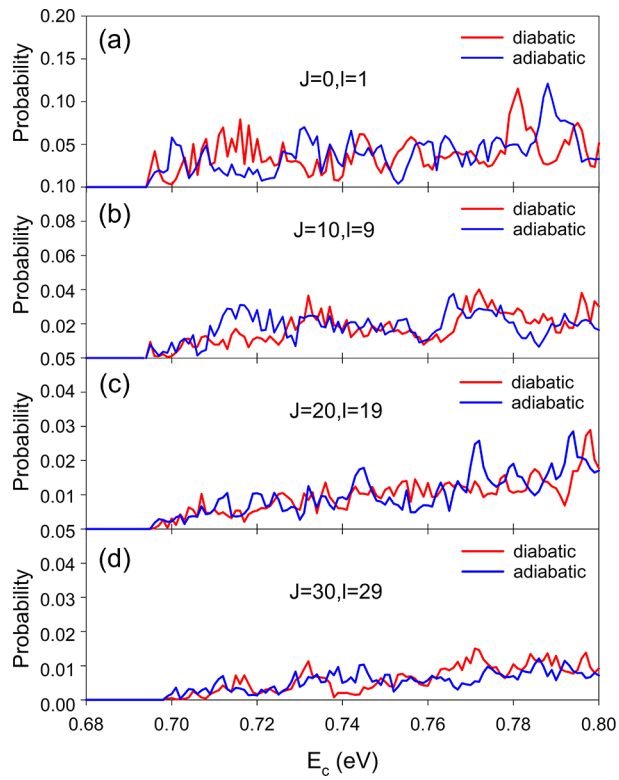

Figure 2. Total reaction probabilities for the reaction H + O_2 (v = 0, j = 1) → O + OH for several partial waves; the red and blue lines show the diabatic and adiabatic results, respectively.

several partial waves. It is clear that the reaction possesses a threshold at 0.695 eV, which well matches the experimental reaction energy (0.72 ± 0.07 eV),[78] underscoring the endoergicity of the reaction. The reaction probabilities strongly oscillate apparently due to metastable resonances supported by the deep HO_2 well. Although the average magnitudes of reaction probabilities are similar, quantitative differences are found between adiabatic and diabatic results even as the collision energies are far below the minimum energy crossing of the CI, which is 1.69 eV above the H + O_2 asymptote.[76] Specifically, the inclusion of the GP in the diabatic results significantly alters the position, width, and amplitude of the resonance peaks in the probabilities. For several energy regions, the GP and NGP results appear to be out of phase. A similar phenomenon was found in probabilities for the H + O_2 inelastic scattering.[62] The reaction probability typically

https://doi.org/10.1021/acs.jpclett.4c00789
J. Phys. Chem. Lett. 2024, 15, 4237−4243

decreases with the increase of the total angular momentum J due to the increasing centrifugal barrier but remains oscillatory. The GP effect is also remarkable at higher J partial waves.

The GP effect displayed in the reaction probabilities seems to be stronger than several previously studied reactive systems. For the activated H + H_2 exchange reaction, the GP effect on probabilities is only significant when the collision energy approaches the energy of the CI.[79,80] For the H + $H_2^+ \rightarrow H_2^+$ + H reaction in its lowest triplet state, which has three equally shallow (0.37 eV) potential wells, the GP effect causes only relatively small changes in total reaction probabilities.[81]

The excitation function, namely, the energy dependence of the ICS, is displayed in Figure 3 up to 0.80 eV. The differences

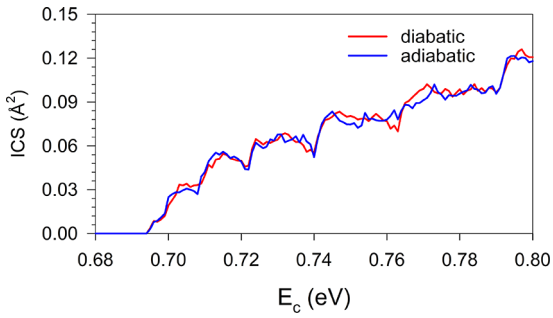

Figure 3. Excitation functions for the reaction H + O_2 (v = 0, j = 1) → O + OH.

between the diabatic and adiabatic ICSs are much less pronounced than the probabilities shown in Figure 2. The sum over partial waves apparently washes away much of the strong oscillations in the reaction probabilities and the GP effects become less pronounced. Unlike the H + H_2 exchange reaction in which the GP effects are completely washed away in ICS,[55,80,82,83] some small but distinguishable effects still remain for the title reaction.

The calculated final state resolved DCSs at E_c = 0.70 eV are plotted in Figures 4(a) and 4(b). The inclusion of GP clearly alters the angular distribution, but at this energy, the differences are small, except in the forward and backward directions. The relative differences in Figure 4(c) show that the GP effect on the DCS for OH (v = 0, j = 0) is larger than that for OH (v = 0, j = 1). In addition, strong oscillations are found in both DCSs at some scattering angles. The GP effect could be understood as the interference between the direct path (labeled as path 1) and looping path (labeled as path 2), which are topologically distinct.[54] In the quantum mechanical framework, results along the two paths could be extracted from linear combinations of the GP and NGP scattering amplitudes (eq 1a).[83,84] The difference between the DCSs obtained from the GP and NGP calculations arises from the interference between two paths, which could be calculated through the sum of the third and fourth terms in eq 1b:

$$f_{\text{path1}}(E) = (f_{\text{NGP}}(E) + f_{\text{GP}}(E))/\sqrt{2}$$
$$f_{\text{path2}}(E) = (f_{\text{NGP}}(E) - f_{\text{GP}}(E))/\sqrt{2} \quad (1a)$$

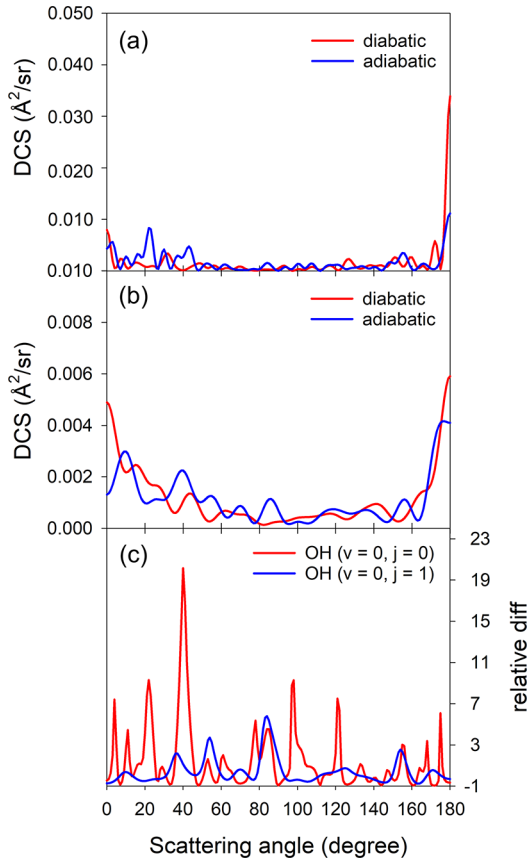

Figure 4. Calculated adiabatic and diabatic DCSs at E_c = 0.70 eV for different final states (a and b) and the relative difference between GP and NGP results (c).

$$\sigma_{\text{NGP}} = (|f_{\text{path1}}(E)|^2 + |f_{\text{path2}}(E)|^2 + (f_{\text{path1}}(E)f^*_{\text{path2}}(E) + f^*_{\text{path1}}(E)f_{\text{path2}}(E)))/2$$
$$\sigma_{\text{GP}} = (|f_{\text{path1}}(E)|^2 + |f_{\text{path2}}(E)|^2 - (f_{\text{path1}}(E)f^*_{\text{path2}}(E) + f^*_{\text{path1}}(E)f_{\text{path2}}(E)))/2 \quad (1b)$$

To illustrate the two topologically distinct paths in the title rection, we perform quasi-classical trajectory (QCT) calculations on the adiabatic ground state PES using VENUS.[85] As shown in Figure 1(b), two typical paths (direct and looping) lead to the same products. In the direct path, the trajectory passes through the HO_bO_a well and reaches the HO_b + O_a product asymptote. In the looping path, on the other hand, the trajectory first passes the HO_aO_b well and then isomerizes to the HO_bO_a well before reaching the HO_b + O_a product asymptote. The isomerization transition state is located at γ = 90°, R = 1.74 bohr, and r_{OO} = 2.69 bohr. The two paths form a complete encirclement of the C_{2v} CI.

The DCSs along the two paths (associated with $|f_{\text{path1}}|^2$, $|f_{\text{path2}}|^2$) and the interference terms (associated with $f_{\text{path1}}(E)f^*_{\text{path2}}(E) + f^*_{\text{path1}}(E)f_{\text{path2}}(E)$) are shown in Figure 5. As mentioned before, the deep potential wells trap the wave functions for a long time, which leads to comparable strengths for the direct and looping paths.[84] As shown in Figure 5, the DCSs along both paths are oscillatory and largely forward–backward symmetric, consistent with the complex-forming character of the reaction. In addition, the GP effects are found

https://doi.org/10.1021/acs.jpclett.4c00789
J. Phys. Chem. Lett. 2024, 15, 4237−4243

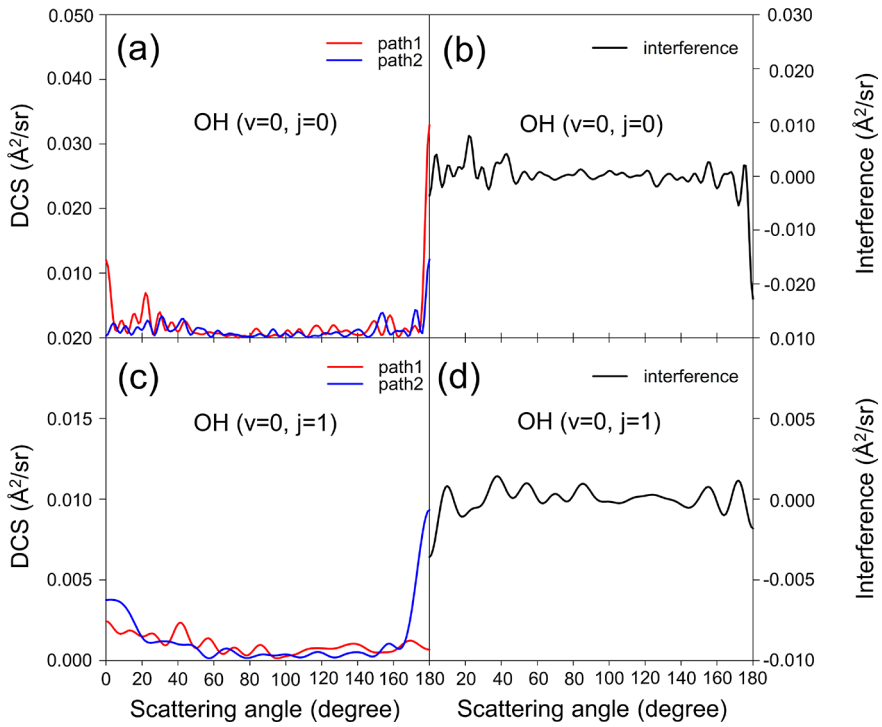

Figure 5. DCSs of the direct (path 1) and looping (path 2) paths at E_c = 0.70 eV for different final states (a and c) and the corresponding interference terms (b and d).

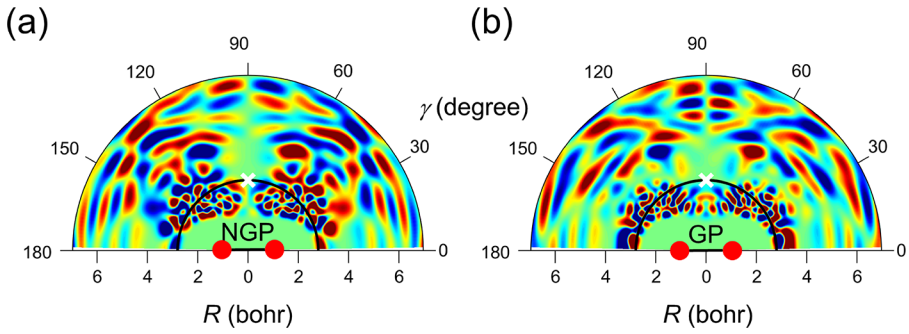

Figure 6. Ground state scattering wave function (J = 0) at E_c = 0.70 eV with r_{OO} (illustrated as the distance between the red balls) fixed at 2.50 bohr, obtained from adiabatic (a) and diabatic (b) calculations. The cross denotes the location of the C_{2v} CI, and the black circle passing through the CI defines the two regions with small and large R.

to be pronounced at most scattering angles, as shown in Figure 4 for both the j = 0 and j = 1 products, suggesting the strong interferences between the two paths along the scattering angles. The GP will affect the positions and widths of resonances as featured by the differences in GP and NGP reaction probabilities, thus leading to a pronounced GP effect in DCS. However, the integration of the DCS over the scattering angle washes away much of the GP effect.

The ICSs for path 1 and path 2 at a collision energy of 0.70 eV were calculated. Since the scattering calculations for extracting the S-matrix are quite challenging due to the large size of grids and very long Chebyshev propagation, we only computed the S-matrix at this energy. It is found that the ICS of the direct path (path 1) 0.0242 Å^2 is slightly larger than that (0.0184 Å^2) of the loop path (path 2), suggesting the competition between the two paths.

To obtain further mechanistic insights into the GP effect in the reaction, we show in Figure 6 the ground state scattering wave function at E_c = 0.70 eV obtained from both the diabatic and adiabatic calculations. The former was obtained from the diabatic wave functions via the AtD transformation to facilitate the comparison. The existence of a deep well supports numerous resonance states, as shown in Figure 2, which produce many nodes in the scattering wave function, as shown in Figure 6. Since the branching space of the C_{2v} CI is spanned by R and γ, the wave functions are plotted in these two coordinates. One of the unique signatures of GP is the wave function that encircles the CI changes its sign.[54] This is reflected here by a change of the permutational symmetry when passing through the CI from the small to large R regions.[86] As shown in Figure 6(b), the GP scattering wave function obtained from the diabatic representation is symmetric with respect to the exchange of the two O nuclei in the small R region, but it becomes antisymmetric outside the CI with a node at γ = 90°. This illustrates the interference between the two paths on opposite sides of the CI.[58] However, this interference feature is absent in the NGP wave function, as shown in Figure 6(a).

https://doi.org/10.1021/acs.jpclett.4c00789
J. Phys. Chem. Lett. 2024, 15, 4237−4243

To summarize, we investigate in this work the impact of GP on the quantum state resolved H + O_2 reactive scattering by comparing adiabatic and diabatic calculations using the same DPEM constructed recently based on high-level ab initio data. Our results suggest that the inclusion of the GP quantitatively changes the reaction probabilities for all partial waves. However, these differences are largely washed out in the ICS, after the DCS is integrated over the scattering angle. Detailed analysis found that the two topologically distinct paths around the CI, i.e., the direct and looping paths, make comparable contributions to the cross sections, and the interference between the two paths leads to a significant impact on the differential cross sections. These insights advance our understanding of GP beyond directly activated reactions.

■ ASSOCIATED CONTENT

Supporting Information

The Supporting Information is available free of charge at https://pubs.acs.org/doi/10.1021/acs.jpclett.4c00789.

Details of the quantum dynamics methods and parameters used in the calculations (PDF)

■ AUTHOR INFORMATION

Corresponding Authors

Changjian Xie − *Institute of Modern Physics, Shaanxi Key Laboratory for Theoretical Physics Frontiers, Northwest University, Xi'an, Shaanxi 710127, China;* orcid.org/0000-0002-2062-430X; Email: chjxie@nwu.edu.cn

Xixi Hu − *Kuang Yaming Honors School, Institute for Brain Sciences, Jiangsu Key Laboratory of Vehicle Emissions Control, Center of Modern Analysis, Nanjing University, Nanjing, Jiangsu 210023, China; Hefei National Laboratory, Hefei, Anhui 230088, China;* orcid.org/0000-0003-1530-3015; Email: xxhu@nju.edu.cn

Hua Guo − *Department of Chemistry and Chemical Biology, Center for Computational Chemistry, University of New Mexico, Albuquerque, New Mexico 87131, United States;* orcid.org/0000-0001-9901-053X; Email: hguo@unm.edu

Daiqian Xie − *Institute of Theoretical and Computational Chemistry, Key Laboratory of Mesoscopic Chemistry, School of Chemistry and Chemical Engineering, Nanjing University, Nanjing, Jiangsu 210023, China; Hefei National Laboratory, Hefei, Anhui 230088, China;* orcid.org/0000-0001-7185-7085; Email: dqxie@nju.edu.cn

Author

Junyan Wang − *Institute of Theoretical and Computational Chemistry, Key Laboratory of Mesoscopic Chemistry, School of Chemistry and Chemical Engineering, Nanjing University, Nanjing, Jiangsu 210023, China*

Complete contact information is available at: https://pubs.acs.org/10.1021/acs.jpclett.4c00789

Notes

The authors declare no competing financial interest.

■ ACKNOWLEDGMENTS

This work was supported by the National Natural Science Foundation of China (Grants 22233003 and 22241302 to D.X., 22073073 to C.X., and 22122302 and 22073042 to X.H.). H.G. is supported by the Department of Energy (Grant DE-SC0015997). This work was also supported by the Innovation Program for Quantum Science and Technology (2021ZD0303305 to D.X.). J.W. thanks Prof. Shanyu Han, Prof. Bin Zhao, and Dr. Hailin Zhao for advice on quantum dynamics calculations. All calculations were performed in the High-Performance Computing Center (HPCC) at Nanjing University.

■ REFERENCES

(1) Miller, J. A.; Kee, R. J.; Westbrook, C. K. Chemical-kinetics and combustion modeling. *Annu. Rev. Phys. Chem.* **1990**, *41*, 345−387.

(2) Walch, S. P.; Duchovic, R. J. Theoretical characterization of the potential energy surface for H+O_2 = HO_{2*} = OH+O. III. Computed points to define a global potential energy surface. *J. Chem. Phys.* **1991**, *94*, 7068−7075.

(3) Guo, H. Quantum dynamics of complex-forming bimolecular reactions. *Int. Rev. Phys. Chem.* **2012**, *31*, 1−68.

(4) Kleinermanns, K.; Linnebach, E. Experimental study of H + O_2 reaction dynamics at collision energies of 2.6, 1.9, and 1.0 eV. *J. Chem. Phys.* **1985**, *82*, 5012−5018.

(5) Pirraglia, A. N.; Michael, J. V.; Sutherland, J. W.; Klemm, R. B. A flash photolysis-shock tube study of the H atom reation with O_2: H + O_2 ⇌ OH + O (962 K < T < 1705 K) and H + O_2 + Ar → HO_2 + Ar (746 K < T < 987 K). *J. Phys. Chem.* **1989**, *93*, 282−291.

(6) Kleinermanns, K.; Linnebach, E.; Pohl, M. Dynamical bottleneck in the reaction H + O_2 → OH + O at high collision energies. *J. Chem. Phys.* **1989**, *91*, 2181−2189.

(7) Bronikowski, M. J.; Zhang, R.; Rakestraw, D. J.; Zare, R. N. Reaction dynamics of H+O_2 at 1.6 eV collision energy. *Chem. Phys. Lett.* **1989**, *156*, 7−13.

(8) Shin, K. S.; Michael, J. V. Rate constants for the reactions H+O_2 → OH+O and D+O_2 → OD+O over the temperature range 1085−278 K by the laser photolysis-shock tube technique. *J. Chem. Phys.* **1991**, *95*, 262−273.

(9) Jacobs, A.; Volpp, H. R.; Wolfrum, J. Absolute reactive cross sections for the reaction H + O_2 → OH + O. *Chem. Phys. Lett.* **1991**, *177*, 200−206.

(10) Kessler, K.; Kleinermanns, K. H + O_2 → OH + O: excitation functions and absolute reaction cross sections. *J. Chem. Phys.* **1992**, *97*, 374−377.

(11) Ryu, S.-O.; Hwang, S. M.; Rabinowitz, M. J. Shock tube and modeling study of the H + O_2 = OH + O reaction over a wide range of composition, pressure, and temperature. *J. Phys. Chem.* **1995**, *99*, 13984−13991.

(12) Fei, R.; Zheng, X. S.; Hall, G. E. Consequences of conical intersections in the H + O_2 → OH + O reaction? *J. Phys. Chem. A* **1997**, *101*, 2541−2545.

(13) Abu Bajeh, M.; Goldfield, E. M.; Hanf, A.; Kappel, C.; Meijer, A. J. H. M.; Volpp, H.-R.; Wolfrum, J. Dynamics of the H + O_2 → O + OH chain-branching reaction: Accurate quantum mechanical and experimental absolute reaction cross sections. *J. Phys. Chem. A* **2001**, *105*, 3359−3364.

(14) Melius, C. F.; Blint, R. J. The potential energy surface of the HO_2 molecular system. *Chem. Phys. Lett.* **1979**, *64*, 183−189.

(15) Miller, J. A. Collision dynamics and the thermal rate coefficient for the reaction H + O_2 → OH + O. *J. Chem. Phys.* **1981**, *74*, 5120−5132.

(16) Kleinermanns, K.; Schinke, R. Dynamics of H+O_2 → OH+O at high collision energies. *J. Chem. Phys.* **1984**, *80*, 1440−1445.

(17) Miller, J. A. Nonstatistical effects and detailed balance in quasiclassical trajectory calculations of the thermal rate coefficient for O+OH → O_2+H. *J. Chem. Phys.* **1986**, *84*, 6170−6177.

(18) Pastrana, M. R.; Quintales, L. A. M.; Brandao, J.; Varandas, A. J. C. Recalibration of a single-valued double many body expansion potential energy surface for ground state HO_2 and dynamics calculations for the O+OH → O_2+H reaction. *J. Phys. Chem.* **1990**, *94*, 8073−8088.

(19) Varandas, A. J. C.; Brandao, J.; Pastrana, M. R. Quasiclassical trajectory calculations of the thermal rate coefficients for the reactions H(D)+O_2 → OH(D)+O and O+OH(D) → O_2+H(D) as a function of temperature. *J. Chem. Phys.* **1992**, *96*, 5137−5150.
(20) Varandas, A. J. C. Excitation function for H+O_2 reaction: A study of zero-point energy effects and rotational distributions in trajectory calculations. *J. Chem. Phys.* **1993**, *99*, 1076−1085.
(21) Pack, R. T.; Butcher, E. A.; Parker, G. A. Accurate quantum probabilities and threshold behavior of the H+O_2 combustion reaction. *J. Chem. Phys.* **1993**, *99*, 9310−9313.
(22) Leforestier, C.; Miller, W. H. Quantum mechanical calculation of the rate constant for the reaction H+O_2 → OH+O. *J. Chem. Phys.* **1994**, *100*, 733−735.
(23) Zhang, D. H.; Zhang, J. Z. H. Quantum reactive scattering with a deep well: Time-dependent calculation for H+O_2 reaction and bound state characterization for HO_2. *J. Chem. Phys.* **1994**, *101*, 3671−3678.
(24) Pack, R. T.; Butcher, E. A.; Parker, G. A. Accurate three-dimensional quantum probabilities and collision lifetimes of the H +O_2 combustion reaction. *J. Chem. Phys.* **1995**, *102*, 5998−6012.
(25) Kendrick, B.; Pack, R. T. Potential energy surfaces for the low-lying 2A″ and 2A′ states of HO_2: use of the diatomics in molecules model to fit ab initio data. *J. Chem. Phys.* **1995**, *102*, 1994−2012.
(26) Dai, J.; Zhang, J. Z. H. Time-dependent wave packet approach to state-to-state reactive scattering and application to H + O_2 reaction. *J. Phys. Chem.* **1996**, *100*, 6898−6903.
(27) Viel, A.; Leforestier, C.; Miller, W. H. Quantum mechanical calculation of the rate constant for the reaction H + O_2 → OH + O. *J. Chem. Phys.* **1998**, *108*, 3489−3497.
(28) Meijer, A. J. H. M.; Goldfield, E. M. Time-dependent quantum mechanical calculation on H+O_2 for total angular momentum J > 0. *J. Chem. Phys.* **1998**, *108*, 5404−5413.
(29) Meijer, A. J. H. M.; Goldfield, E. M. Time-dependent quantum mechanical calculation on H+O_2 for total angular momentum J > 0 II: On the importance of Coriolis coupling. *J. Chem. Phys.* **1999**, *110*, 870−880.
(30) Goldfield, E. M.; Meijer, A. J. H. M. Time-dependent quantum mechanical calculations on H + O_2 for total angular momentum J > 0. III. Total cross sections. *J. Chem. Phys.* **2000**, *113*, 11055−11062.
(31) Zhang, H.; Smith, S. C. Chebyshev real wave packet propagation: H + O_2 (J = 0) state-to-state reactive scattering calculations. *J. Chem. Phys.* **2002**, *117*, 5174−5182.
(32) Sultanov, R. A.; Balakrishnan, N. Quantum scattering calculations of the H + O_2 → O + OH reaction. *J. Phys. Chem. A* **2004**, *108*, 8759−8764.
(33) Xu, C.; Xie, D.; Zhang, D. H.; Lin, S. Y.; Guo, H. A new ab initio potential energy surface of $HO_2(X^2A'')$ and quantum studies of HO_2 vibrational spectrum and rate constants for the H + O_2 ↔ O + OH reactions. *J. Chem. Phys.* **2005**, *122*, 244305.
(34) Lin, S. Y.; Guo, H.; Honvault, P.; Xie, D. Quantum dynamics of the H + O_2 → O + OH reaction on an accurate ab initio potential energy surface. *J. Phys. Chem. B* **2006**, *110*, 23641−23643.
(35) Lin, S. Y.; Rackham, E. J.; Guo, H. Quantum mechanical rate constants for H + O_2 ↔ O + OH and H + O_2 → HO_2 reactions. *J. Phys. Chem. A* **2006**, *110*, 1534−1540.
(36) Honvault, P.; Lin, S. Y.; Xie, D.; Guo, H. Differential and integral cross sections for the H + O_2 → OH + O combustion reaction. *J. Phys. Chem. A* **2007**, *111*, 5349−5352.
(37) Bargueno, P.; Gonzalez-Lezana, T.; Larregaray, P.; Bonnet, L.; Claude Rayez, J. Time dependent wave packet and statistical calculations on the H + O_2 reaction. *Phys. Chem. Chem. Phys.* **2007**, *9*, 1127−1137.
(38) Hankel, M.; Smith, S. C.; Meijer, A. J. H. M. State-to-state reaction probabilities for the H + O_2(v,j) → O + OH(v′,j′) reaction on three potential energy surfaces. *J. Chem. Phys.* **2007**, *127*, No. 064316.
(39) Xie, D.; Xu, C.; Ho, T.-S.; Rabitz, H.; Lendvay, G.; Lin, S. Y.; Guo, H. Global analytical potential energy surfaces for $HO_2(X^2A'')$ based on high level ab initio calculations. *J. Chem. Phys.* **2007**, *126*, 074315.
(40) Lendvay, G.; Xie, D.; Guo, H. Mechanistic insights into the H + O_2 → OH + O reaction from quasi-classical trajectory studies on a new ab initio potential energy surface. *Chem. Phys.* **2008**, *349*, 181−187.
(41) Lin, S. Y.; Sun, Z.; Guo, H.; Zhang, D. H.; Honvault, P.; Xie, D.; Lee, S.-Y. Fully Coriolis coupled quantum studies of the H + O_2 → OH + O reaction on an accurate potential energy surface: integral cross sections and rate constants. *J. Phys. Chem. A* **2008**, *112*, 602−611.
(42) Sun, Z.; Zhang, D. H.; Xu, C.; Zhou, S.; Xie, D.; Lendvay, G.; Lee, S.-Y.; Lin, S. Y.; Guo, H. State-to-state dynamics of H + O_2 reaction. Evidence for nonstatistical behavior. *J. Am. Chem. Soc.* **2008**, *130*, 14962−14963.
(43) Lin, S. Y.; Guo, H.; Lendvay, G.; Xie, D. Effects of reactant rotational excitation on the H + O_2 → OH + O reaction rate constant: Quantum wave packet, quasi-classical trajectory, and phase space theory calculations. *Phys. Chem. Chem. Phys.* **2009**, *11*, 4715−4721.
(44) Quéméner, G.; Kendrick, B. K.; Balakrishnan, N. Quantum dynamics of the H+O_2→O+OH reaction. *J. Chem. Phys.* **2010**, *132*, 014302.
(45) Varandas, A. J. C. Accurate combined-hyperbolic-inverse-power-representation of ab initio potential energy surface for the hydroperoxyl radical and dynamics study of O+OH reaction. *J. Chem. Phys.* **2013**, *138*, 134117.
(46) Szabó, P.; Lendvay, G. Dynamics of complex-forming bimolecular reactions: A comparative theoretical study of the reactions of H atoms with $O_2(^3\Sigma_g^-)$ and $O_2(^1\Delta_g)$. *J. Phys. Chem. A* **2015**, *119*, 12485−12497.
(47) Ghosh, S.; Sharma, R.; Adhikari, S.; Varandas, A. J. C. 3D time-dependent wave-packet approach in hyperspherical coordinates for the H + O_2 reaction on the CHIPR and DMBE IV potential energy surfaces. *Phys. Chem. Chem. Phys.* **2018**, *20*, 478−488.
(48) Ghosh, S.; Sharma, R.; Adhikari, S.; Varandas, A. J. C. Fully coupled (J > 0) time-dependent wave-packet calculations using hyperspherical coordinates for the H + O_2 reaction on the CHIPR potential energy surface. *Phys. Chem. Chem. Phys.* **2019**, *21*, 20166−20176.
(49) Yarkony, D. R. Diabolical conical intersections. *Rev. Mod. Phys.* **1996**, *68*, 985−1013.
(50) Domcke, W.; Yarkony, D. R.; Köppel, H. *Conical Intersections: Electronic Structure, Dynamics and Spectroscopy*; World Scientific: Singapore, 2004.
(51) Mead, C. A.; Truhlar, D. G. On the determination of Born−Oppenheimer nuclear motion wave functions including complications due to conical intersections and identical nuclei. *J. Chem. Phys.* **1979**, *70*, 2284−2296.
(52) Longuet-Higgins, H. C.; Öpik, U.; Pryce, M. H. L.; Sack, R. A. Studies of the Jahn-Teller effect. II. The dynamical problem. *Proc. Royal Soc. A (London)* **1958**, *244*, 1−16.
(53) Berry, M. V. Quantal phase factors accompanying adiabatic changes. *Proc. Royal Soc. A (London)* **1984**, *392*, 45−57.
(54) Mead, C. A. The geometric phase in molecular systems. *Rev. Mod. Phys.* **1992**, *64*, 51−85.
(55) Kendrick, B. K. Geometric phase effects in chemical reaction dynamics and molecular spectra. *J. Phys. Chem. A* **2003**, *107*, 6739−6756.
(56) Althorpe, S. C.; Juanes-Marcos, J. C.; Wrede, E. The influence of the geometric phase on reaction dynamics. *Adv. Chem. Phys.* **2008**, *138*, 1−42.
(57) Ryabinkin, I. G.; Joubert-Doriol, L.; Izmaylov, A. F. Geometric phase effects in nonadiabatic dynamics near conical intersections. *Acc. Chem. Res.* **2017**, *50*, 1785−1793.
(58) Xie, C.; Malbon, C. L.; Guo, H.; Yarkony, D. R. Up to a sign. The insidious effects of energetically inaccessible conical intersections on unimolecular reactions. *Acc. Chem. Res.* **2019**, *52*, 501−509.

https://doi.org/10.1021/acs.jpclett.4c00789
J. Phys. Chem. Lett. 2024, 15, 4237−4243

(59) Ryabinkin, I. G.; Izmaylov, A. F. Geometric phase effects in dynamics near conical intersections: Symmetry breaking and spatial localization. *Phys. Rev. Lett.* **2013**, *111*, 220406.
(60) Xie, C.; Ma, J.; Zhu, X.; Yarkony, D. R.; Xie, D.; Guo, H. Nonadiabatic tunneling in photodissociation of phenol. *J. Am. Chem. Soc.* **2016**, *138*, 7828−7831.
(61) Yuan, D.; Guan, Y.; Chen, W.; Zhao, H.; Yu, S.; Luo, C.; Tan, Y.; Xie, T.; Wang, X.; Sun, Z.; et al. Observation of the geometric phase effect in the H + HD → H_2 + D reaction. *Science* **2018**, *362*, 1289−1293.
(62) Kendrick, B.; Pack, R. T. Geometric phase effects in H+O_2 scattering. II. Recombination resonances and state-to-state transition probabilities at thermal energies. *J. Chem. Phys.* **1996**, *104*, 7502−7514.
(63) Kendrick, B.; Pack, R. T. Geometric phase effects in H+O_2 scattering. I. Surface function solutions in the presence of a conical intersection. *J. Chem. Phys.* **1996**, *104*, 7475−7501.
(64) Kendrick, B.; Pack, R. T. Geometric phase effects in the resonance spectrum, state-to-state transition probabilities and bound state spectrum of HO_2. *J. Chem. Phys.* **1997**, *106*, 3519−3539.
(65) Kendrick, B. K.; Hazra, J.; Balakrishnan, N. The geometric phase controls ultracold chemistry. *Nat. Commun.* **2015**, *6*, 7918.
(66) Hazra, J.; Kendrick, B. K.; Balakrishnan, N. Importance of geometric phase effects in ultracold chemistry. *J. Phys. Chem. A* **2015**, *119*, 12291−12303.
(67) Huang, J.; Kendrick, B. K.; Zhang, D. H. Mechanistic insights into ultracold chemical reactions under the control of the geometric phase. *J. Phys. Chem. Lett.* **2021**, *12*, 2160−2165.
(68) Meek, G. A.; Levine, B. G. Wave function continuity and the diagonal Born-Oppenheimer correction at conical intersections. *J. Chem. Phys.* **2016**, *144*, 184109.
(69) Smith, F. T. Diabatic and adiabatic representations for atomic collision problems. *Phys. Rev.* **1969**, *179*, 111−123.
(70) Guo, H.; Yarkony, D. R. Accurate nonadiabatic dynamics. *Phys. Chem. Chem. Phys.* **2016**, *18*, 26335−26352.
(71) Mead, C. A.; Truhlar, D. G. Conditions for the definition of a strictly diabatic electronic basis for molecular systems. *J. Chem. Phys.* **1982**, *77*, 6090−6098.
(72) Baer, M. Adiabatic and diabatic representations for atom-molecule collisions: Treatment of the collinear arrangement. *Chem. Phys. Lett.* **1975**, *35*, 112−118.
(73) Yarkony, D. R. Nonadiabatic quantum chemistry - past, present and future. *Chem. Rev.* **2012**, *112*, 481−498.
(74) Guan, Y.; Xie, C.; Yarkony, D. R.; Guo, H. High-fidelity first principles nonadiabaticity: Diabatization, analytic representation of global diabatic potential energy matrices, and quantum dynamics. *Phys. Chem. Chem. Phys.* **2021**, *23*, 24962−24983.
(75) Shu, Y.; Varga, Z.; Kanchanakungwankul, S.; Zhang, L.; Truhlar, D. G. Diabatic states of molecules. *J. Phys. Chem. A* **2022**, *126*, 992−1018.
(76) Wang, J.; An, F.; Chen, J.; Hu, X.; Guo, H.; Xie, D. Accurate full-dimensional global diabatic potential energy matrix for the two lowest-lying electronic states of the H + O_2 ↔ HO + O reaction. *J. Chem. Theory Comput.h* **2023**, *19*, 2929−2938.
(77) Guo, H.. Chebyshev propagation and applications to scattering problems. In *Theory of Chemical Reaction Dynamics*, Lagana, A., Lendvay, G.. Eds.; Kluwer, 2004; pp 217−229.
(78) Litorja, M.; Ruscic, B. A photoionization study of the hydroperoxyl radical, HO_2, and hydrogen peroxide, H_2O_2. *J. Electron Spectrosc. Relat. Phenom.* **1998**, *97*, 131−146.
(79) Bouakline, F.; Althorpe, S. C.; Peláez Ruiz, D. Strong geometric-phase effects in the hydrogen-exchange reaction at high collision energies. *J. Chem. Phys.* **2008**, *128*, 124322.
(80) Kendrick, B. K. Geometric phase effects in the H + D_2 → HD + D reaction. *J. Chem. Phys.* **2000**, *112*, 5679−5704.
(81) He, H.; Xu, H.; Chen, L.; Xie, P.; Yin, S. Geometric phase effects in the H + H_2^+ Reaction on the lowest triplet ground state. *J. Phys. Chem. A* **2023**, *127*, 9966−9973.
(82) Carlos Juanes-Marcos, J.; Althorpe, S. C. On the role of the conical intersection in H+H_2 reactive scattering. *Chem. Phys. Lett.* **2003**, *381*, 743−750.
(83) Juanes-Marcos, J. C.; Althorpe, S. C.; Wrede, E. Theoretical study of geometric phase effects in the hydrogen-exchange reaction. *Science* **2005**, *309*, 1227−1230.
(84) Althorpe, S. C. General explanation of geometric phase effects in reactive systems: Unwinding the nuclear wave function using simple topology. *J. Chem. Phys.* **2006**, *124*, No. 084105.
(85) Hase, W. L.; Duchovic, R. J.; Hu, X.; Komornicki, A.; Lim, K. F.; Lu, D.-H.; Peslherbe, G. H.; Swamy, K. N.; Linde, S. R. V.; Varandas, A.; et al. VENUS96: A General Chemical Dynamics Computer Program. *Quantum Chemistry Program Exchange Bulletin* **1996**, *16*, 671.
(86) Barclay, V. J.; Dateo, C. E.; Hamilton, I. P.; Kendrick, B.; T Pack, R.; Schwenke, D. W. Anomalous symmetries of the rovibrational states of HO_2: Consequences of a conical intersection. *J. Chem. Phys.* **1995**, *103*, 3864−3867.

https://doi.org/10.1021/acs.jpclett.4c00789
J. Phys. Chem. Lett. 2024, 15, 4237−4243